Lifetime-Extended MCP-PMT

T. Jinno[a], T. Mori[a], T. Ohshima[a], Y. Arita[a], K. Inami[a], T. Ihara[b], H. Nishizawa[b], and T. Sasaki[b]

[a] *Department of Physics, Nagoya University, Chikusa, Nagoya 464-8602, Japan*
[b] *Hamamatsu Photonics K.K. Electron Tube Division Manuf.#1, Dept.43, 314-5 Shimokanzo, Iwata, Shizuoka 438-0193, Japan*

Abstract

In order to develop a long-lifetime MCP-PMT under high rates of circumstance, we investigated the degradation of the quantum efficiency (QE) of PMT's with a multialkali photocathode. We found that not only positive ions, but also neutral residual gases would damage the photocathode resulting in an enhancement of the work function; their countermeasures were established in newly manufactured square-shaped MCP-PMT's with 4 or 4×4 multi-anodes. The performances of the PMT's were measured: QE was stable up to an integrated amount of anode output charge of $2-3$ C/cm^2, while keeping other basic performances steady, such as the time resolution for single photons ($\sigma_{\rm TTS}$) of $\simeq 40$ ps, a photoelectron collection efficiency (CE) of 60%, a multiplication gain (G) of a few $\times 10^6$, and dark counts of $20-300$ Hz. The causes of QE degradation are discussed.

Keywords: MCP-PMT, Photocathode, QE, Lifetime, TOP counter

1. Introduction

The most difficult R&D item of a microchannel plate (MCP) photo-multiplier tube (PMT) is to settle the subject for protecting the photocathode from its QE degradation under a high counting rate for a long experimental period.

We previously found [1, 2] that an Aluminum prevention layer from ion-feedbacks plays an essential role for this problem, and an MCP-PMT (Hamamatsu Photonics K.K. (HPK) R3809U-50-11X) with a multialkali photocathode kept its performance up to the integrated amount of output charge of $Q > 2.6$ C/cm^2, corresponding to more than a 14-year time duration [3] under our supposed Super-KEKB/Belle-II [4].

Our development of MCP-PMT's for the practical use on a newly proposed K/π particle identification detector, a time-of-propagation (TOP) counter [5], was then followed, in order to enlarge its effective area, change its cross section from circular to square-shaped and to equip it with multi-anodes. The characteristics and performance of the developed MCP-PMT, SL10, are satisfactory, as reported in [2]. However, unexpected

Email address: mori@hepl.phys.nagoya-u.ac.jp (T. Mori)

QE degradation, which brings the above work to naught, was encountered after the previous publication.

While studying photocathodes, such as bi-alkali, multialkali, and GaAs(P) materials, including a negative electron affinity (NEA) property, has in general long-continued, their details and certain understandings have not been established due to complexity from a solid-state physics viewpoint. Especially investigations of the QE deterioration of photocathodes in the case of MCP-PMT are scarce. We carried out an exhaustive study on this phenomenon, by manufacturing about 30 different versions of MCP-PMT's. The resulting SL10 with a $Na_2KSb(Cs)$ multialkali photocathode survived up to $Q = 2-3$ C/cm^2. It could satisfactory perform well over 10 equivalent-years at the Super-KEKB/Belle-II. New insights were gained, about which we would like to report here.

We hereafter refer to MCP-PMT as simply PMT, for brevity.

2. PMT and Setups

2.1. SL10

While the basic characteristics of the SL10 can be found in Table 1 in [2], slight variations were made for individual SL10 versions in this research. Table 1 is presented for the reader's convenience.

2.2. Setup for a QE degradation measurement

The QE degradation of PMT's is measured in terms of an integrated amount of output charge, $\sum_{\rm Q}$, by the system, illustrated in Fig.1 in [1]. The system consists of an LED, a light pulser, a filter, a standard PMT for calibration, and PMT's tested, in a black box. An LED ($\lambda \simeq 400$ nm) was pulsed (10 ns-wide) at repetition rates of $f = 1-20$ kHz, which yielded the number of observed photoelectrons, $N_{\rm p.e.} = 20-50$ per pulse, corresponding to the output charge from an anode of $\sum_{\rm Q} = 2-10$ mC/cm^2/day under an expected Belle-II condition, $\sum_{\rm Q}$=0.16 C/cm^2 per year. During continuous irradiation, the performance of SL10's for single photons was monitored every 1-3 days, using a light pulser PLP ($\lambda = 408$ nm with a duration of 50 ps (FWHM) and a jitter of $\pm$10 ps).

2.3. Setup for a QE λ-dependence measurement

To measure the $QE(\lambda)$-spectrum, a monochromator system was prepared by a Halogen lamp, a monochromator ($\lambda = 350-900$ nm) with a wavelength-cut filter, a Si photodiode as a standard photo-device, and a pico-ampere meter to measure the photocurrents, as illustrated in Fig.5 in [1].

3. Al Prevention Layer

It was concluded in our previous study that the QE deterioration of the photocathode could be attributed to positive ion-feedbacks, produced in the multiplication process of secondary electrons. The bias-angle setting of the MCP might not be powerful enough as a single measure of ion-feedbacks. We succeeded to protect the photocathode from ion-feedbacks by equipping a thin Aluminum layer between the photocathode and the 1st MCP-layer. The effect of the Al-layer was proved upon removing the after-pulses due

Table 1: Basic characteristics of SL10. Some variations can be found, compared to Table 1 in [2].

items	SL10
photocathode	multialkali $Na_2KSb(Cs)$
window	borosilicate glass
effective area	22×22 (mm^2)
QE @ $\lambda = 400$ nm	~ 20 (%)
channel-diameter of MCP	10 (μm)
length-to-diameter ratio of MCP	40
MCP aperture	~ 60 (%)
bias angle	$13(^o)$
Al prevention layer ♯	ON
anodes	4, 4×4
	gap (mm) / voltage (kV) ♭
photocathode - 1st MCP	2.0 / 0.2
1st MCP in - out	0.4 / 1.0
1st - 2nd MCP's	1.0 / 1.0
2nd MCP in - out	0.4 / 1.0
2nd MCP - anodes	1.0 / 0.6
HV supplied	3.4-3.8 (kV)
gain	$(1-3)\times10^6$
σ_{TTS}	30-40 (ps)
dark counts	$\mathcal{O}(10-10^4)$ (Hz)
CE	60 (%)

♯ For the effect of Al prevention layer, see the text and Table 2.

♭ Placing the Al prevention layer on the 2nd MCP yields a distance of 1 mm between MCP's.

to ion-feedbacks, and the QE of the photocathode at 400 nm for a PMT R3809U-50-11X had remained stable for a longer period of $\sum_{\mathrm{Q}} > 2.6$ C/cm^2.

3.1. CE and Al-layer

The drawback of introducting an Al prevention layer is a reduction of the photoelectron collection efficiency (CE) to $\sim 35\%$ from $\sim 60\%$ in the case of no Al-layer, as can be seen in Table 2. CT0790 and YA0071 are R3809U-50-11X circular-shaped PMT's, used in a previous study, but they were made especially for this research. The CT0790 has an Al-layer between the photocathode and 1st-MCP, and the YA0071 does not.

In order to optimize the Al-layer positioning, two different SL10's of YJ-versions were prepared with a 4×4 anode configuration. The YJ0006 equips the Al-layer between the photocathode and the 1st MCP, and the YJ0011 has it between the 1st and 2nd MCP-layers. In the latter case, 1 mm of distance between the MCP's was prepared, and a HV was applied between them.

The YJ0006 exhibits $CE = 36\%$, just as the CT0790 does, while the YJ0011 results in $CE = 60\%$, the maximum efficiency, which is equivalent to the MCP aperture of SL10 in the case of no Al-layer.

Based on this study, all SL10's manufactured ever since are equipped with an Al-layer between the MCP-layers.

Table 2: Al-layer effect on CE

item	R3809U-50-11X		SL10	
PMT	CT0790	YA0071	YJ0006	YJ0011
window	synthetic silica		borosilicate glass	
external size (mm^3)	$45^{\phi} \times 70.2$		27.5×27.5×12.1	27.5×27.5×13.1
effective area (mm^2)	11^{ϕ}		22×22	
Al layer	cathode-1st MCP	No	cathode-1st MCP	1st-2nd MCP
anode	single		4×4	
HV (v)	3,400		3,240	3,420
$QE(@\lambda = 400$ nm) (%)	21	19	$9^{\sharp}$	23
CE (%)	37	65	36	60
Gain ($\times 10^6$)	1.5	1.9	0.41	1.1
TTS (ps)	29	34	37	35
dark counts (kcps)	1.5	0.38	0.04	2.1

$\sharp$: Photocathode was not successfully made, so that QE was low but CE measurement would not be influenced.

3.2. SL10 and lifetime $\tau_{\rm Q}$

For our convenience, we define the lifetime, $\tau_{\rm Q}$, in terms of $\sum_{\rm Q}$, at which the QE drops to 80% ($\simeq -1$ dB) of the beginning. Within this QE limit, the performance of the TOP counter could remain unaffected.

Figure 1 shows the observed QE vs. $\sum_{\rm Q}$ variation of the CT0790 and YJ0011 PMT's. The CT0790 exhibits a long life of $\tau_{\rm Q} > 3$ C/cm^2, as expected from previous measurements; however, it showed a small degradation that was not detected for the previous CT0790 up to $\sum_{\rm Q} \simeq 3$ C/cm^2.

Concerning the YJ0011, one of the most corner located (1st) and one of the central (6th) anodes among the 4×4 configuration (numbered in sequence from a corner) are plotted. In spite of furnishing the Al-layer, the YJ0011 exhibited a much shorter lifetime of $\tau_{\rm Q} = 0.03 - 0.05$ C/cm^2, compared to the CT0790. The fact that the 1st-anode drops QE faster than the 6th-anode is also observed (but not plotted) for the YJ0006.

We measured the QE distribution over the photocathode surface on YJ0011 by scanning with a slit of 1×1 mm^2-size using a monochromator system at $\lambda = 400$ nm; Fig.2 shows the observed distributions before and after full irradiation of $\sum_{\rm Q} \simeq 0.065$ C/cm^2. The QE distribution is quite homogeneous at the beginning, while it degrades, especially, further along the surrounding. For instance, it varies from $QE \simeq 23-24\%$ to $\simeq 10-17\%$ at the vicinity of the center and from $20 - 24\%$ to $\sim 5\%$ along the sides.

For the CT0790, the Al-layer essentially functions to protect the photocathode, but this is not the case for the SL10. There might exist another source(s) of deterioration.

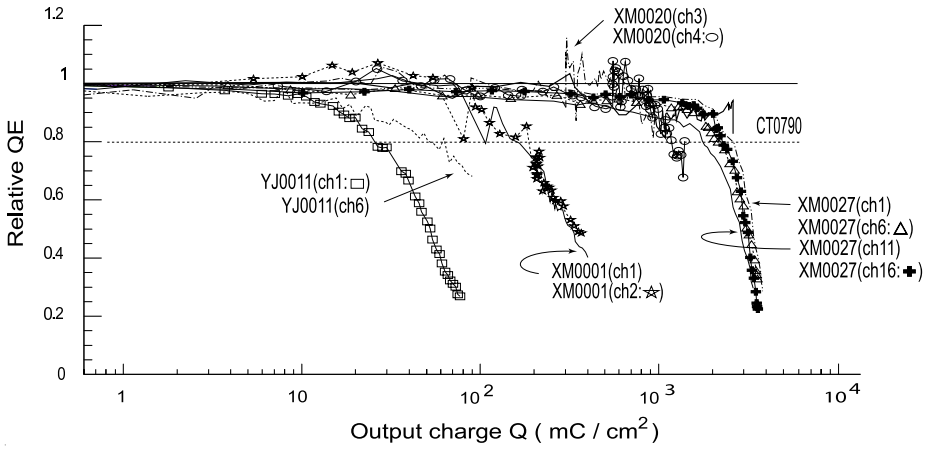

Fig. 1: Relative QE vs. $\sum_{\mathrm{Q}}$. Plotted are for R3809U-50-11X (CT0790) and SL10's (YJ0011, XM0001, XM0020 and XM0027).

3.3. Inner structure and residual gases

Fig.3 illustrates the inner structure of two kinds of PMT's. The CT0790 holds MCP-layers adhered to a cylindrical ceramic container. On the other hand, the container of the SL10 is made of a cubic shape of metal in order to have sufficient mechanical strength to sustain a wider effective area, and its MCP-layers are held with different supporting parts for YJ0011.

We speculate that some neutral molecular residual gases exist, bounced from the MCP's in the multiplication process of the secondary electrons, and whose production rate is proportional to the $\sum_{\mathrm{Q}}$, just the same as the production rate of the positive-ions, which will damage the photocathode. Even so, it is expected that the residual gases are prevented by the Al-layer, just as the positive-ions are. It is inferred that it might be for the gases passing through the MCP channels to the photocathode, but it might not be for the gases making a detour through the side-ways between the MCP's and the metallic wall. As discussed later, gases such as carbon dioxide and monoxide, oxygen, and water, which can be the main ingredients of the residual gases, are reported to affect the work function, ϕ, of the photocathodes.

Our research has since then focused on two subjects. One is to confirm the above conjecture concerning neutral residual gases; the other is to find measures to cope with their suppressions or removal.

4. Suppression of Gases

4.1. Sealing photocathode from gases

We have manufactured various different SL10's, named as JT-versions (its structure is essentially the same as that of YJ0011, as listed in Table 1 and 2, but with 4 anode-channels), each of which replaces some elements that attempt to suppress the residual

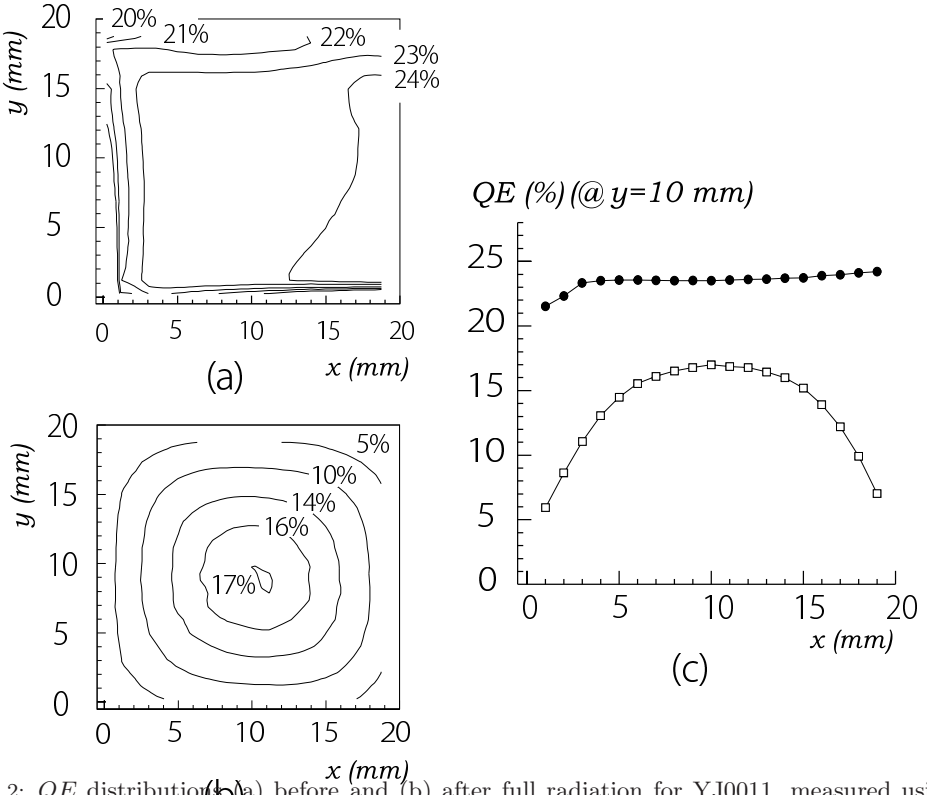

Fig. 2: QE distributions (a) before and (b) after full radiation for YJ0011, measured using a monochromator system with $\lambda = 400$ nm. (c) shows the QE x-distributions before (●) and after (□) at y=10 mm.

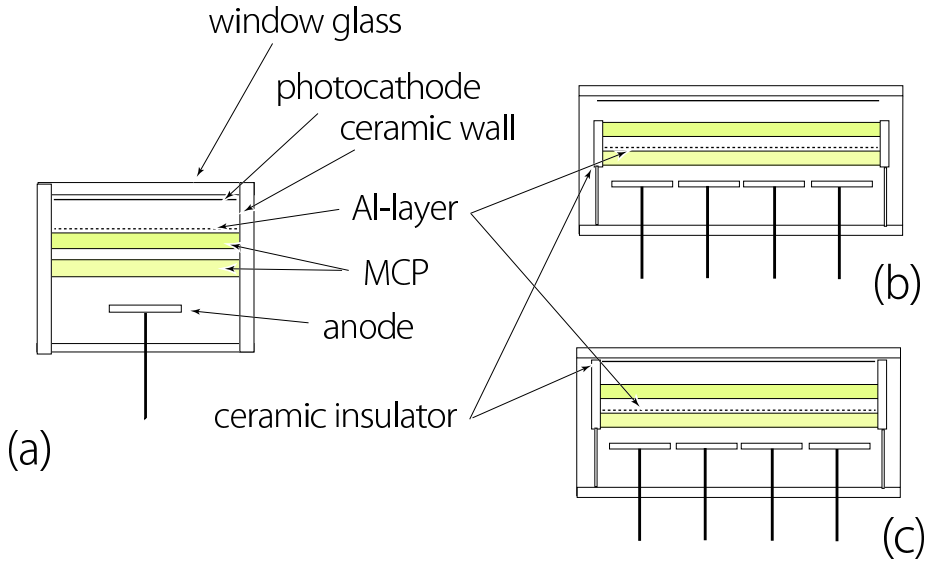

Fig. 3: Schematic drawing of inner structure of PMT's. (a) CT0790, (b) YJ0011 and (c) XM-versions. Arrows for common items are omitted for (b) and (c).

gases. Among many trails, for examples, MCP's are replaced with ones of different material-property; MCP's are electron-scrubbed to further remove the residual gases; getters are furnished close to the photocathode to adsorb out-gases, and so on. No improvement in the lifetime has been obtained for any of the PMT's: $\tau_{\rm Q} < 0.1$ C/cm^2.

Next, we employed ceramic elements, on the one hand, to support MCP-layers (Fig.3(b) and (c)) and, on the other hand, to isolate the photocathode from the gap-space between the MCP's and metal-walls where the gases would be supposed to pass through (Fig.3(c)). These SL10's are named "XM-version", and the insulation becomes tighter with the XM-version number. The lifetime now extends to $\tau_{\rm Q} \sim 0.1$ C/cm^2 by XM0001. We have found after many examinations that the tighter is the ceramic isolation, the longer is the lifetime attained.

Supposing that the MCP's are the source of residual gases outbreaking, MCP's are further treated to the highest degree of cleanliness, as mentioned above, in addition to furnishing the Al prevention layer between the MCP's. The SL10 has been developed with a succession of its manufacturing, and the longest lifetime now reaches $\tau_{\rm Q} = 2 - 3$ C/cm^2 by XM0027.

4.2. Gases vs. ion-feedback

In developing the XM-version, at an early stage we attained a lifetime of $\tau_{\rm Q} = 0.1 - 1$ C/cm^2. The XM0001, having 4 anodes, is such a PMT (see, Fig.1). Their QE's of all 4-anodes drop to 70-80% after irradiation of $\sum_{\rm Q} \simeq 0.2$ C/cm^2 (see, Fig.4(a)); since then, half of its photocathode-surface ($y \geq 12$ mm), corresponding to the 3rd and 4th anode-channels, is shielded from irradiating light. If the QE drop can be attributed, regardless of the Al-layer presence, to positive-ions or something else produced in the

multiplication process and feedback through the MCP channels, the degradation over the shielded surface will stop. We, of course, do not observe the output signals from these anodes at the rates of the LED triggered, but do so from the 1st and 2nd anodes.

Observation for a consecutive irradiation of $\sum_{\rm Q} \simeq 0.16$ C/cm^2 results in a quite similar QE degradation, as can be seen in Fig.4(b), with the former one. Table 3 also lists the QE drops for 4 anodes in the cases with and without half shielding. The QE drops $\sim 20\%$ more in the surrounding than that in the center area.

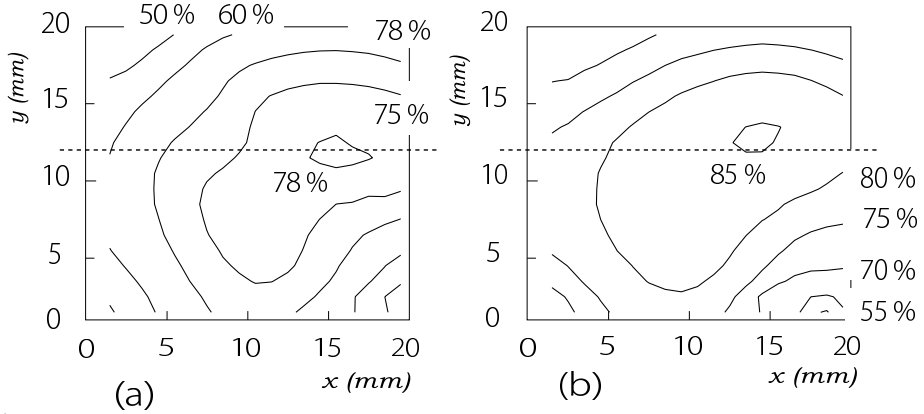

Fig. 4: Contours of QE drops for XM0001, measured with $\lambda = 400$ nm. The integrated output charge, $\sum_{\rm Q}$, over the irradiation period is (a) $\simeq 0.2$ C/cm^2 and (b) $\simeq 0.16$ C/cm^2. For (b) half of the photocathode surface ($y \geq 12$ mm), corresponding to the 3rd and 4th anodes, is shielded from the light.

Table 3: QE drops for 4-anodes of XM0001 in cases of the photocathode surface, fully opened and half (3rd and 4th) shielded, respectively, after irradiation of $\sum_{\rm Q} \simeq 0.2$ C/cm^2 and $\simeq 0.16$ C/cm^2. Measurements were made with $\lambda = 400$ nm, and the observed QE error was evaluated to be $\pm 1\%$.

anode channel	1st	2nd	3rd	4th
Full-opened (%)	68	71	71	63
Half-shielded (%)	71	83	85	76

This fact supports our speculation that the residual gases taking the roundabout route, not directly through the MCP channels, to the photocathode would cause QE deterioration.

5. SL10 with $\tau_Q \sim 2 - 3$ C/cm^2

Along with steady progress by improving the individual elements and mechanical structure, we have obtained insulation-tight SL10's, the XM0020 and XM0027 with 4 and 4×4 anodes, respectively, which attain $\tau_{\rm Q} \simeq 1$ and $2 - 3$ C/cm^2, as can be seen in

Fig. 1. The lifetime of the XM0027 is the longest one ever achieved, which corresponds to $12 - 19$ equivalent-years at the planed Super-KEKB / Belle-II.

Homogeneous photocathode manufacturing on the square-shaped window has been established. No strong degradation along the sides has been observed for these SL10's, as shown in Fig. 5.

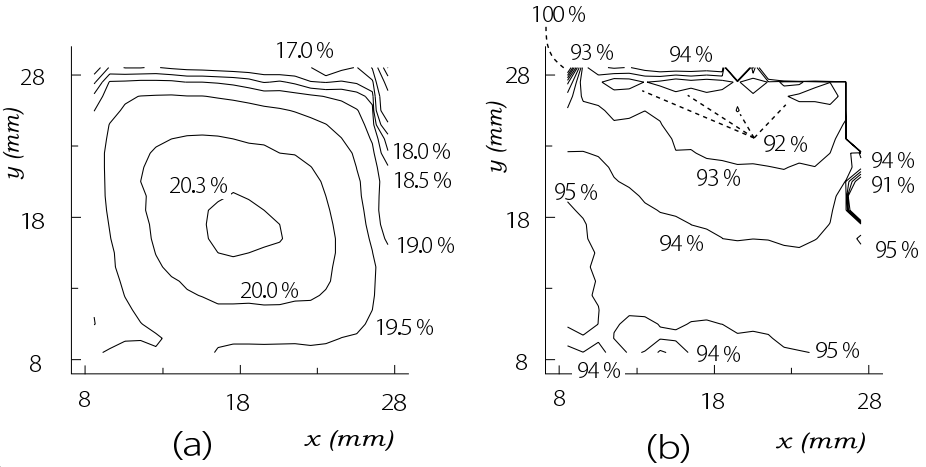

Fig. 5: Distributions of (a) the initial QE and (b) the QE drop after irradiation of $\sum_{\rm Q} \simeq 0.36$ C/cm^2 for XM0020, measured with $\lambda = 400$ nm.

Figure 6 shows their performance: the output signals for single photons, the ADC and TDC histograms for the XM0020, and the relative gain variation and the time resolutions, $\sigma_{\rm TTS}$, for the XM0027 during the irradiation. The gain is $G \sim (1-3) \times 10^6$ in the beginning, but it linearly drops with $\sum_{\rm Q}$. For instance, it is reduced to 60% at $\sum_{\rm Q} = 3.8$ C/cm^2 for the XM0027 (HV=3.8 kV). The $\sigma_{\rm TTS}$ value is stable, and exhibits a similar value between the two XM's; it varies within a range of 41 ± 4 (ps) for the XM0027 and within 46 ± 4 (ps) for the XM0020.

Dark counts of the XM0020 (HV=3.8 kV) are $\sim$ 18 kHz at the 2nd anodes, but $\sim$ 1 kHz at the other 3 anodes in the beginning, while they are $\sim$ 3 kHz, but $\sim$ 10 Hz, respectively, after the irradiation period. A similar situation also occurs for the XM0027. They are 16, 36, 160 and 330 Hz at the 1st, 2nd, 3rd and 4th anodes in the beginning, and 0.2, 3, 4 and 17 Hz after irradiation.

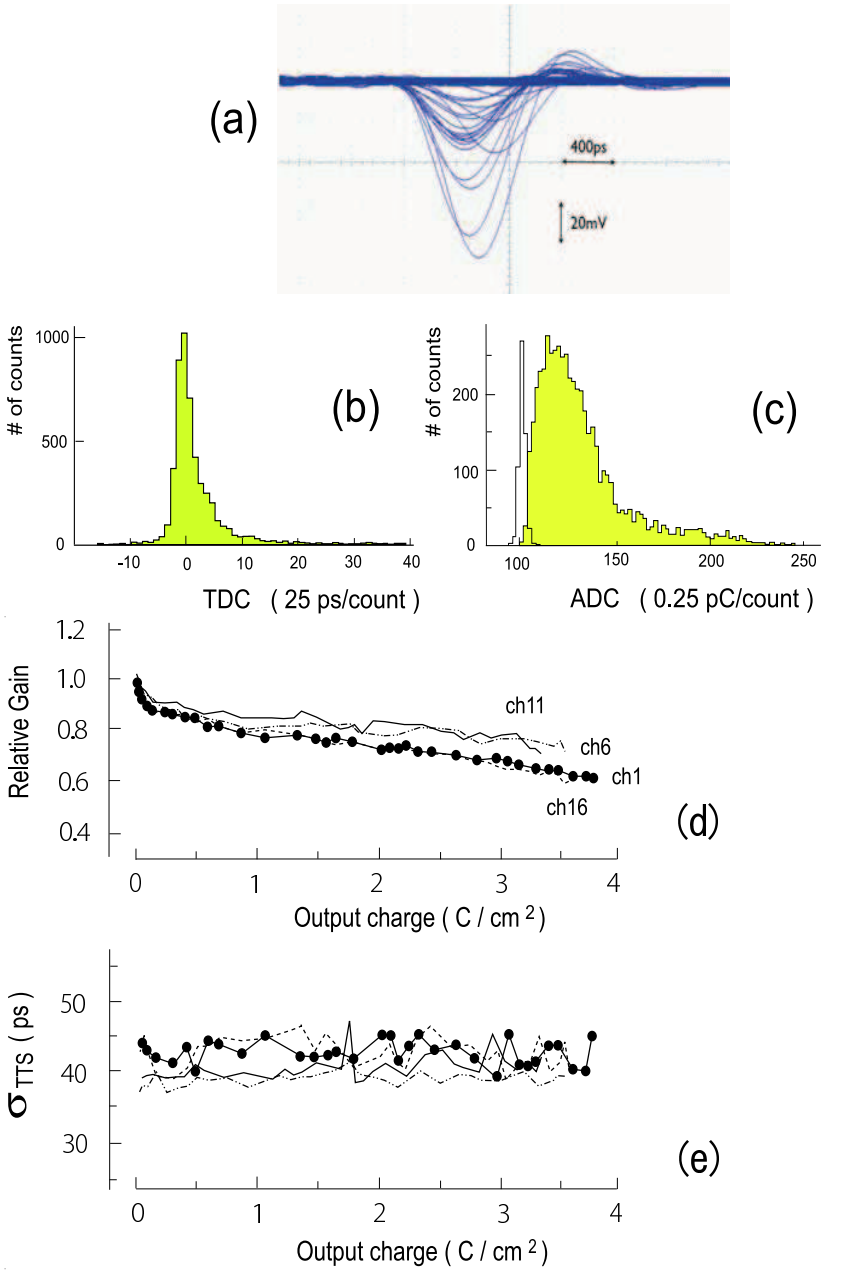

Fig. 6: Performance of XM0020 and XM0027. (a) output signals, (b) TDC and (c) ADC distributions for XM0020, measured with HV=3,400 kV. (d) and (e) are the relative gain variation and the time resolution for single photons for XM0027.

6. Discussions and Results

6.1. Effect on the work function

The photoelectron emission consists of four consecutive processes. The absorption of a photon ($E = h\nu$) by the cathode material, the excitation of a valence electron to the conduction band, transfer of the excited electron to the cathode-surface, and the emission of an electron in a vacuum [6]. QE is a product of the probabilities of these processes, and it is cut-off at a shorter wavelength of $\lambda \sim 300$ nm for borosilicate glass, fixed by the transmittance index of a window material, and at a longer wavelength of $\lambda \sim 900$ nm, settled by the work function ($\phi \simeq 1.4$ eV of the multialkali $Na_2KSb(Cs)$ photocathode).

As can be seen in Fig.7(a), an irradiation of $\sum_{\rm Q} \simeq 0.2$ C/cm^2 on the XM0001 induces a shift of the longer wavelength-cutoff. The ϕ value changes from 1.4 eV ($\lambda \simeq 900$ nm) to $\simeq 1.7$ eV ($\simeq 700$ nm). The XM0020, on the other hand, keeps QE stable, even at $\sum_{\rm Q} \simeq 0.36$ C/cm^2 (see, Fig.7(b)).

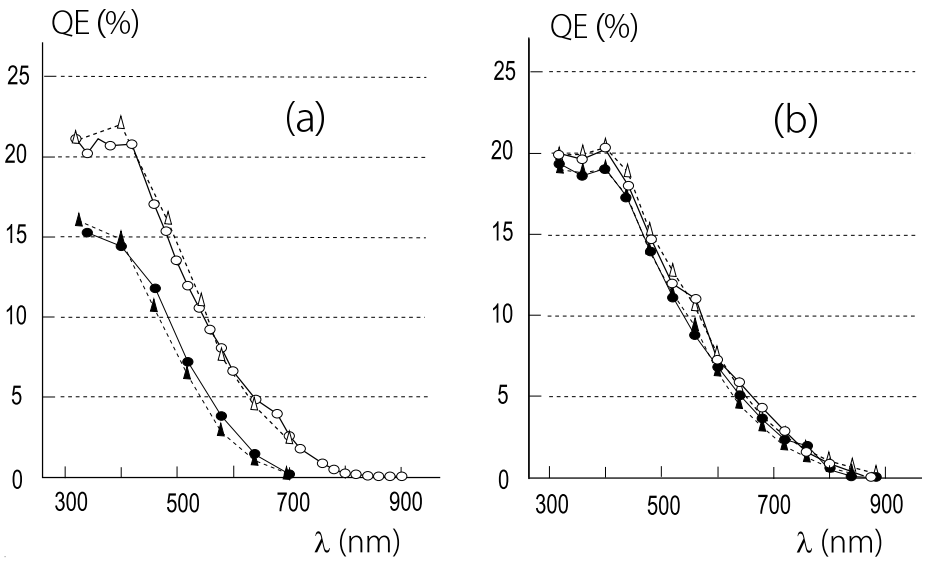

Fig. 7: QE(λ) spectrum changes: (a) XM0001 with $\sum_{\rm Q} = 0.2$ C/cm^2 and (b) XM0020 with $\sum_{\rm Q} = 0.36$ C/cm^2. $\circ$ and $\triangle$ are for the 1st and 2nd anodes at the beginning, and $\bullet$ and $\blacktriangle$ after irradiation.

6.2. Cause of QE degradation

Let us itemize, without any prejudice, what we found concerning the cause:

(1) Furnishing an Al-layer makes it possible to extend the lifetime, $\tau_{\rm Q}$, by about two orders of magnitude, or more than that without the layer for the R3809U-50-11X. The Al-layer cuts across the inner structure between the photocathode and the 1st MCP, and it eliminates the after-pulse signals from the anodes [1].

(2) For SL10, while the Al-layer also splits the inner structure into two (but between the MCP-layers), there still remains a gap-space between the MCP's and the container. Unless this gap-space is covered, an extension of the lifetime cannot be accomplished.

(3) Without covering the gap-space, the photocathode reduces its QE over the whole area; the reduction is strong, especially along the sides of the container. Although half of the photocathode-surface is shaded from irradiating photons, QE degradation occurs at the shaded area, just as the un-shaded region is affected. Covering the gap space extends the QE lifetime to as long as $\tau_{\rm Q} = (2-3)$ C/cm^2.

(4) High degrees of cleaning and degassing of MCP-layers to reduce residual gases helps to improve the lifetimes.

We previously conjectured positive-ion feedbacks to be the cause of QE degradation. However, from the above-observed facts we now presume that the previous conjecture is not a unique explanation. Residual gases are also the cause. Moreover, it is possibly the main reason.

6.3. Gases and photocathode's molecular structures

We so far speculate that neutral residual gases bounced from the MCP-layers are the cause of QE degradation. There are several reports on the effect of some gases on photocathodes. T. Wada *et. al.* [7] indicated that CO_2, CO and H_2O gases influence the QE of (NEA) GaAs photocathodes, among which CO_2 molecules seem to have a serious influence; also P. Michelato *et. al.* [8] have reported that CO_2 and O_2 gases produce a rapid QE drop for KCsSb bi-alkali photocathodes, but CH_4 and CO gases are sufficiently harmless. They measured the QE change as a function of the exposure time duration under certain gas pressures; however, we do not have any information about the pressure and residual gases of our PMT's.

Our brief interpretation of the data by T. Wada *et. al.* [7] points out that the CO_2 or O_2 gases could yield an appreciable QE degradation when the photocathode is exposed to the gas in terms of the product of its pressure and exposure duration of $\mathcal{O}(\geq 10^{-10})$ (Torr$\times$h). By applying this criterion for our SL10, we estimate the gas pressure, p, when it arrives at its lifetime, $\tau_{\rm Q}$. The residual gases in our case are accumulated with time, so that the resulting effect would appear to be proportional to $\sum_{\rm Q} \times t$, where t is the full time-length since the beginning of irradiation. An order evaluation suggests $p \sim \mathcal{O}(10^{-13})$ (Torr) for the XM0027.

C. Ghosh and B. P. Varma [9] studied alkali antimonide photocathodes, and measured the work functions to be $\phi \sim 1.4$ eV for Na_2KSb(Cs) and 1.8 eV ($\lambda \simeq 680$ nm), 1.9 eV ($\lambda \simeq 650$ nm) and 2.2 eV ($\lambda \simeq 560$ nm) for Na_2KSb, K_2SbCs and K_3Sb structures, respectively. Accordingly, the variations of our $QE(\lambda)$ and λ-cutoff before and after a large irradiation might indicate a change in the photocathode structure from that of conventional Na_2KSb(Cs) to Na_2KSb. They have the same band-gap of 1.1 eV, but their work functions are different by ~ 0.4 eV.

T. Guo and H. Gao [10] have discussed rules concerning cesium and oxygen on the energy levels of several kinds of photocathodes. An excess of oxygen will reside on top of the Cs activation-layer, resulting in a $Na_2KSb-Cs-O$ structure rather than the nominal $Na_2KSb-O-Cs$ structure, and then increase ϕ and decrease QE.

6.4. Ideal measure

It is acceptable to think that the Al-layer, made by evaporating Aluminum to a few ten's of $\mathring{A}$-thick, could substantially prevent positive ions and residual gases from passing through. Our R3809U-50-11X still does not show any obvious QE-drop up to $\sum_{\rm Q} \simeq 3$ C/cm^2.

Besides the Al-layer, although the insulation of the gap-space from the photocathode is done in the case of SL10, it is not air-tight, but rather black-outing, so that the gases could leak into the photocathode domain, and might lead to a QE drop, as observed.

Accordingly, the most ideal way would be to realize the inner structure to be the same as the R3809U-50-11X. Both mechanical and electric considerations must be required. If it can be materialized, the lifetime could be extended to be much longer than that of XM0027.

6.5. Aging

It has been found that some PMT's exhibit rapid decreases of QE and G in the first $\sum_{\rm Q} \sim 0.1$ C/cm^2. It drops by $5-10\%$, which can be seen in Fig.6(d) on G. The gain, G, also slowly decreases linearly with $\sum_{\rm Q}$, and a similar behavior occurs concerning the rate of the dark counts, mentioned in the previous section for XM0020 and XM0027.

All of those effects might be ascribed to aging phenomena of the PMT. Its effect is most remarkable for the dark counts. Their rates decrease by about two orders of magnitude during irradiation.

6.6. Results

As a photo-device for the TOP counter, planned for the second generation of the high-luminosity B-factory Super-KEKB/Belle-II, we have developed an MCP-PMT, SL10, having considerable endurance under high rates of counting for a long experimental period. It is found that in addition to positive ion-feedbacks, residual gases had substantial influences on the lifetime of the PMT. The QE variation with the integrated amounts of the output charge, $\sum_{\rm Q}$, was measured, and the $QE(\lambda)$ spectra before and after irradiation were examined for about 30 different versions of SL10's.

Both the furnishments of the Al-layer and the ceramic-insulation largely suppress the ions and gases from damaging the photocathode, and then resulting in a long lifetime of $\tau_{\rm Q} \simeq 2-3$ C/cm^2, which is equivalent to well more than 10 years of operation at the supposed Super-KEKB/Belle-II.

The resulting SL10 with 4×4 anodes, XM0027, exhibits in a satisfactory performance with $\sigma_{\rm TTS} \simeq 40$ ps, QE($\lambda = 400$ nm)$\simeq 20\%$, CE=60%, G=$(1-3)\times10^6$ and dark counts of $20-300$ Hz.

Acknowledgments

This work is supported by a Grant-in-Aid for Science Research in a Priority Area ("New Development of Flavor Physics") from the Ministry of Education, Culture, Sports, Science and Technology of Japan, and from the Japan Society for the Promotion of Science for Creative Scientific Research ("Evolution of Tau-lepton Physics"). We acknowledge support from the Tau-Lepton Physics Research Center of Nagoya University.

References

[1] N. Kishimoto *et al.*, Nucl. Instr. and Meth. **A564** (2006) 204;
[2] K. Inami *et al.*, Nucl. Instr. and Meth. **A592** (2008) 247.
[3] For the lifetime evaluation we suppose the detector condition with a luminosity of $2 \times 10^{35}/\mathrm{cm}^2/\mathrm{s}$ in the ref.[1], while new condition with $4 \times 10^{35}/\mathrm{cm}^2/\mathrm{s}$ in this time. Also, typical PMT performance is set as CE=50% and $G = 2 \times 10^6$ previously but 60% and 1×10^6 here while keeping QE as 20%. We also take account of actual operation time per year. Therefore, the conversion rate from Q to the experimental equivalent-year is different between two cases.
[4] S. Hashimoto, (ed) *et al.*, Letter of Intent for KEK Super B Factory, KEK-REPORT-2004-4 (jun 2004).
[5] M. Akatsu *et al.*, Nucl. Instr. and Meth. **A 440** (2000) 124-135; T. Ohshima, Nucl. Instr. and Meth. **A 453** (2000) 331-335; T. Ohshima, ICFA Instr. Bull. **20** (2000) 2, (15pages); M. Hirose *et al.*, Nucl. Instr. and Meth. **A 460** (2001) 326-335; S. Matsui *et al.*, Nucl. Instr. and Meth. **A 463** (2001) 220-226; Y. Enari *et al.*, Nucl. Instr. and Meth. **A 494** (2002) 430-435; T. Hokuue *et al.*, Nucl. Instr. and Meth. **A 494** (2002) 436-440; Y. Enari *et al.*, Nucl. Instr. and Meth. **A 547** (2005) 490-503;
[6] W. E. Spicer, Appl. Phys. **12** (1977) 115-130.
[7] T. Wada, T. Nitta, T. Nonura, M. Miyao and T. Nomura, Jap. Jour. App. Phys., **29** (1990) 2087-2091.
[8] P. Michelato, C. Pagani, D. Sertore and S. Valeri, EPAC 94, Fourth European Particle Accelerator Conf., London, 1994, Poster Sessions, 1456.
[9] C. Ghosh and B. P. Varma, J. Appl. Phys. **49** (1978) 4549-4553.
[10] T. Guo and H. Gao, Appl. Surface Science **70/71** (1993) 355-358.